Unsteady forces and flow patterns of the flow around a rectangular cylinder under in-line oscillation

Donglai YI* and Atsushi OKAJIMA**

*Graduate School, Kanazawa University, 2-40-20 Kodatsuno, Kanazawa, Ishikawa, Japan 920
**Dr. of Eng., Professor, Graduate School of Natural Science and Engineering, Kanazawa University, ibid.

It is getting more and more significant to understand the flow about an oscillating bluff body. In this paper we report our experimental and numerical studies on the flow about a rectangular cylinder which is forced to oscillate in-line with a uniform incident flow at amplitude of a/H=14% (H: cross-flow dimension of cylinder section) and at various frequencies. Force measurements made on mean values of drags C_D and *rms* values of lifts C_L at Re=4×10³ show that both C_D and C_L values don't have sharp changes which are experienced by a circular cylinder within the lock-in region of in-line oscillation. Instead, they only show some slight changes. The vortices can shed in different combinations of two source frequencies, i.e., natural shedding frequency f_n and forced oscillatory frequency f_e of the cylinder, and can easily synchronize with the latter. The synchronization range can be divided into two kinds and is much wider than that of a circular cylinder. Visualization is also conducted in a water tank, using the hydrogen bubble method, to show the flow patterns and the effects of in-line oscillation on the wakes. The flows under the same conditions but Re=10³ were two-dimensionally simulated with *DS* (Direct Simulation) method. Both measured forces and visualized flow patterns are presented and discussed together with the two-dimensional simulations.

***Key words**: unsteady flow, wake, rectangular cylinder, in-line oscillation, aerodynamic forces, visualization*

1. Introduction

When one of the inherent frequencies of a bluff body is near the Strouhal frequency at which vortices are naturally shed from corresponding stationary body, the body can undergo vortex-induced oscillation in a direction transverse to or parallel to the incident flow if the damping of the system is sufficiently small. A range of frequencies also exists near the Strouhal frequency of vortex shedding where the induced transverse or in-line oscillation of the body cause the vortex frequency to be captured by, or to synchronize with, the body's oscillatory frequency.

Most investigations on vortex-induced oscillation and its forced-body analogue have concentrated upon vibration transverse to the flow, but vortex-induced oscillation also occurs in the direction in-line with the incident flow. Only recently, some researchers paid their attention on the flow past a cylinder oscillating in-line with a uniform incident flow or a fixed cylinder placed in a pulsating incident flow. Among them are Tanida et al.[1], Griffin & Ramberg[2], Knisely et al.[3], Naudascher[4] and Ongoren & Rochwell[5], Okajima & Kitajima[6] and Minewitsch et al.[7]

Most early studies concerning in-line oscillations were concentrated on circular cylinders. Tanida et al.[1] were probably the earliest to measure the fluctuating lift and mean drag forces for a circular cylinder oscillating in-line with an incident flow. They found that the vortex shedding frequencies synchronize with the oscillating frequency in a range around double the Strouhal frequency. The fluctuating lift and mean drag forces take maxima in the middle of the synchronization range.

On the other hand, King et al.[8,9] studied the free response characteristics in streamwise direction of a circular cylinder and found that there are two regions of excitation. One is within a range of reduced velocities between roughly 1 and 2.5, and the other above 2.5. They also noted two distinct forms of vortex shedding modes, with symmetric shedding prevailing in the first excitation region and antisymmetric shedding the second. Griffin and Ramberg[2] measured the bounds of regime in which the forced vibration of a circular cylinder can control the vortex shedding and cause the lock-in phenomenon. They visualized the flow patterns and found that the two distinct forms of vortex street also exist in the flow around a forced oscillating cylinder.

For rectangular cylinders, Knisely et al.[3] studied the effects of small amplitude perturbations imposed over a mean flow on the pressure coefficients and wake development. With the pulsation frequency equal to twice or four times the natural shedding frequency, the mean base pressure shows a decrease when compared with its value in steady flow. Flow visualization shows this

decease in mean base pressure to be associated with increased vortex strength, decreased vortex formation length, and the corresponding increase in shear layer curvature. When the perturbation amplitude exceeds an undetermined threshold value at a frequency corresponding to four times the natural shedding frequency, two vortices are shed simultaneously and symmetrically with respect to the body center-line.

The most recent study on rectangular cylinders under in-line oscillation is the numerical simulations by Minewitsch et al.[7] They numerically calculated the flow around a square cylinder oscillating in-line with the mean flow at a low Reynolds number Re=200. The unsteady forces on the cylinder are calculated and the interaction of vortex shedding and forced cylinder motion is examined, in particular the occurrence of the lock-in phenomenon. The numerical results lead to the postulation of three regimes for antisymmetric vortex shedding, which was compared with the lock-in regime given out by Griffin and Ramberg[2] for circular cylinder.

In this paper, we measured fluctuating lift and drag forces acting on a rectangular cylinder of different side ratios (B/H=1, 2, 3 where B refers to streamwise dimension of cylinder section and H the cross-flow dimension) which was forced to oscillate in-line with an incident flow at Re=4×10³ and at various Strouhal numbers. Also obtained are the frequencies of vortex shedding and the phase differences of drag forces with respect to cylinder displacements. Visualization is employed to understand the flow patterns and wake structures. Furthermore, the flows under the same conditions but Re=10³ were two-dimensionally simulated with *DS* (Direct Simulation) method, and the simulated results were compared with those of experiments. Parts of simulation results were reported before[10].

2. Experimental Facilities

2.1. Experimental Setup

The experiments were conducted in an open water tank facility, of which the dimensions are 10 meter in length, 70 centimeter in width and 40 centimeter in depth. A platform with an oscillations-generating device upon it can move along the rails of water channel, driven by a DC servomotor of high quality, as shown in Fig.1. The velocity of platform can be regulated by changing the voltage inputted to a servo amplifier. The oscillations-generating device can produce in-line oscillations in the Strouhal number range of 0.0 to 0.5 by using a stepless speed-change motor (rotating speed from 0 to 208 *rpm*). When an axial cam coupled with the stepless speed-change motor rotates, it causes models to vibrate sinusoidally at a certain amplitude which is controlled by a specially designed groove on the surface of the cam.

Three rectangular cylinders of side ratios B/H=1, 2, 3 were used in the experiments with H, which is 30*mm*, facing the upstream flow. The cylinders are 360*mm* in span dimension and made as light as possible to make small the

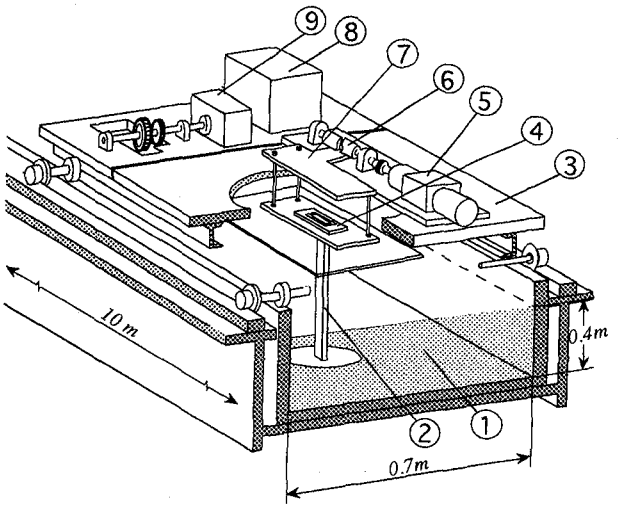

Fig.1. The experimental setup; ①open water tank, ②testing model, ③platform, ④load-cell, ⑤stepless speed-variable motor, ⑥axial cam, ⑦servo amplifier, ⑧DC servomotor

inertia forces of the models. The Reynolds number is Re=4×10³. In all cases, the models are either stationary or forced to oscillate, of which the reduced frequency or forced Strouhal number $St_c(=f_cH/U$, where f_c is the forced frequency and U the velocity of incident flow which equals the speed of the platform) is in a range form 0.0 to 0.5, and the amplitude is a/H=14%.

2.2. Data Measuring and Processing

A load-cell with sensitive semi-conductive gauges (*KYOWA*) building Wheatstone bridge is used to measure fluid forces directly. The load-cell is so designed that it can only measure the forces in one direction in one experimental run with the advantage of being insensitive to the forces in other directions. It should be turned by 90° in order to measure the forces perpendicular to the previous direction. Before the experiment, the load-cell is statically calibrated by attaching weights to the model. The natural frequency of the cylindrical models is above 20*Hz* for all three models, sufficiently high with respect to the phenomenon frequency of the wake flow.

The displacement of model is measured by a Multi-Use Vibration Meter, and the frequency of forced vibration by a circular slit installed on the shaft of the stepless speed-variable motor. Both displacement and force signals were presented to a low-pass filter and then recorded into a personal computer automatically and analyzed on a computer workstation to provide mean value of drag, *rms* value of lift, frequency spectral analyses of lift signals and phase differences of drag forces with respect to cylinder displacements. Before experiments, the inertia forces of the model itself were measured with the cylinders oscillating in still air and then subtracted from the overall forces measured in a uniform incident flow.

Strictly speaking, corrections to the measured data should be made due to the blockage effects from the both side walls. In the present paper, however, no correction was made because there exists no available correction method now for an oscillating rectangular cylinder.

2.3. Flow visualization method

The flows were visualized using hydrogen bubble method, of which one prominent advantage is its ability to get instantaneous flow patterns. The platinum wire generating hydrogen bubble was located about 10*mm* ahead of cylinder. A laser generator was used to produce a laser sheet parallel to water surface to show the flow pattern. A video camera was mounted on the platform to record the fluid motion with respect to the oscillating cylinder. All visualization photos in the present paper were printed out from video tapes using a *UP-1800 SONY* Video Printer.

3. Outline of Numerical Simulations

Fundamental equations of numerical simulations are the Navier-Stokes equations and continuity equation based on assumptions of unsteady, viscous, incompressible and laminar flow. The equations are discretized over elementary control volumes on a body-fitted curvilinear coordinates system. The space derivative terms are discretized by the *QUICK* scheme for convective terms and by the second-order central difference scheme for all other terms. For time marching, the implicit Crank-Nicolson scheme is used. The Poisson equation for a pressure is solved by the Successive-Over-Relaxation (*SOR*) method, and the Navier-Stokes equations are solved to satisfy the continuity equation, following the algorithm of *SIMPLE* method. Corresponding to the forced oscillation of cylinder, the convective terms $(v \cdot \nabla)v$ in Navier-Stokes equations are replaced by $((v-V) \cdot \nabla)v$ where v is the velocity vector of incident flow, and V that of forced oscillation. Boundary conditions are uniform flow at upstream inlet and at upper and lower surfaces of the two dimensional computational domain, zero-gradient flow at downstream exit, and no-slip conditions at surfaces of oscillating cylinder. The simulated results are shown and discussed together with experimental results.

4. Experimental Results

4.1. Unsteady lift and drag forces

Consider a rectangular cylinder oscillating in-line with a uniform incident flow with a displacement of $x(t)=x_0\sin(2\pi f_c t)$, the hydrodynamic lift and drag forces acting on the cylinder are composed of mean values and fluctuating parts. Due to the symmetry of rectangular cylinder, the mean values of lift forces are always zero, so we only present the *rms* values of lifts C_L and mean values of drags C_D for discussion about hydrodynamic forces.

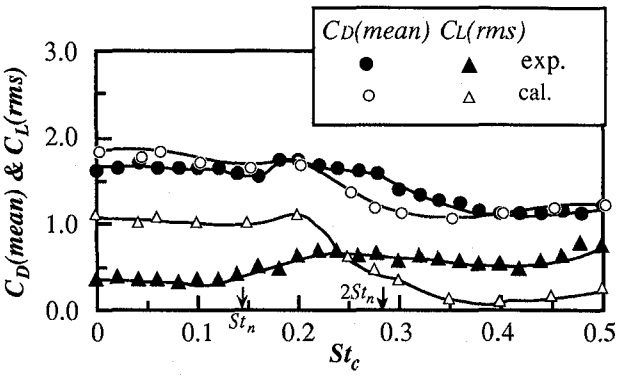

Fig.2. Variations of lifts C_L and drags C_D along forced oscillatory Strouhal number St_c for square cylinder under in-line oscillation at amplitude of a/H=14%

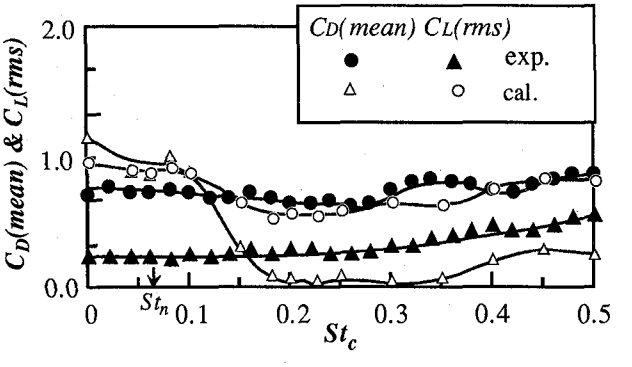

Fig.3. Variations of lifts C_L and drags C_D along forced oscillatory Strouhal number St_c for B/H=2 cylinder under in-line oscillation at amplitude of a/H=14%

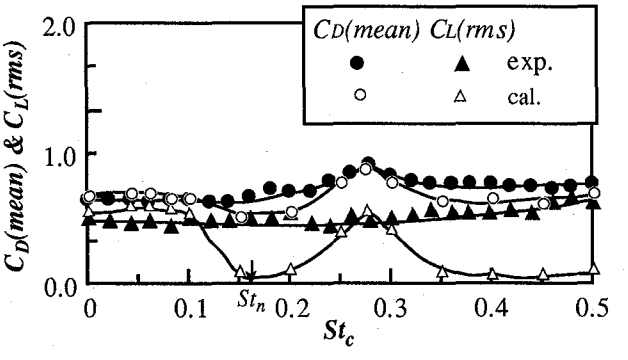

Fig.4. Variations of lifts C_L and drags C_D along forced oscillatory Strouhal number St_c for B/H=3 cylinder under in-line oscillation at amplitude of a/H=14%

Fig. 2 shows the variations of lifts C_L and drags C_D along the forced Strouhal number St_c for square cylinder under in-line oscillations of amplitude a/H=14%. As shown in the legend, the solid circles and triangles represent experimental results and the open ones are simulated results. Also shown in the abscissa is the natural

Strouhal number St_n ($=f_nH/U$; f_n is the natural vortex shedding frequency from stationary cylinder). From the figure it can been seen that the drag forces keep almost constant up to about St_c=0.16, after which the drag forces increase somewhat and then drop to another constant value at about St_c=0.34. Corresponding to this plateau values of C_D, the lift forces seem also have a wide swelling part. Both increases in C_L and C_D are thought to be concerned with such a synchronization region that the vortex shedding frequencies synchronize with half of the forced frequencies and the vortices shed alternatively (as will be discussed in next subtitle). Unlike the case of forced transverse oscillations in which the lift forces increase greatly at high forced frequencies, the lift forces of in-line oscillations don't change that much and only increase a little after St_c> 0.42. Compared with numerical simulations, it can been seen, the C_D curve agrees well with that of experiments, but the C_L curve is some far from satisfaction. Some remarks on comparisons of experimental and simulated results and on reasons of the discrepancy will be given in section 6.

Some interesting comparison can be made between the lift and drag forces acting on a circular and a square cylinder under in-line oscillations. In the literatures, Tanida et al.[1] once measured the lifts and drags acting on an oscillating circular cylinder. They found that the *rms* lifts and mean drags take maxima in the middle of the synchronization range where the vortex shedding frequency synchronizes with the half of forced frequency around double the Strouhal frequency. The peak values increased, respectively, by about 180% and 100% for C_L and C_D. For square cylinder in the present measurements, however, there are only some small increases in C_L and C_D, about 80% and 20% respectively, and the C_D even decreases to a smaller value after the plateau.

The variations of lifts C_L and drags C_D along forced Strouhal number St_c for B/H=2 and 3 cylinders are shown in Figs.3 and 4. The symbols for experimental and simulated results are the same as in Fig.2 and shown in legends. It is confirmed again that the lift forces don't change as much as in transverse oscillation cases; they only increase a little at very high forced Strouhal numbers. For drag forces, there exists a small peak at about St_c=0.35 and 0.28 for B/H=2 and 3 cylinders, respectively. These two peaks also correspond well to the synchronization regions where the vortex shedding frequencies synchronize with half of the forced frequencies and the vortices shed alternatively as shown later in Figs. 6 and 7. Comparing experiments with simulations, we find that, once again, the agreement on C_D curve is relatively good and on C_L curve far from satisfaction. The strict symmetric vortex shedding in simulations, which is not likely to occur in experiments, is responsible for the sharp decreases of lift forces and thus results in the discrepancies (see section 6).

4.2. Frequency components of vortex shedding

Figs.5, 6 and 7 show the variations of vortex shedding

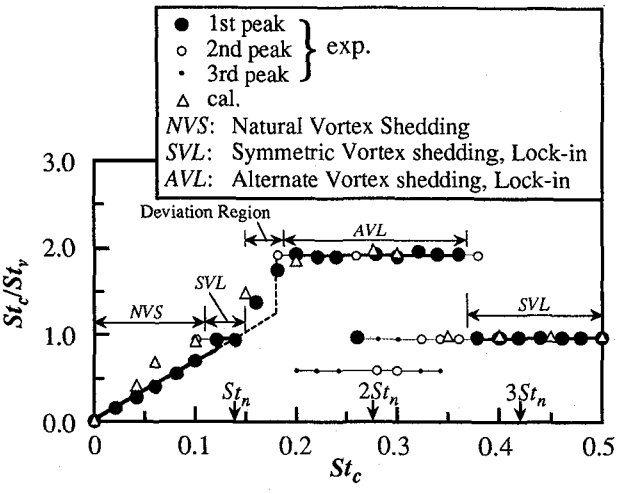

Fig.5. Variation of vortex shedding Strouhal number St_v along forced oscillatory Strouhal number St_c for square cylinder under in-line oscillation at amplitude of a/H=14%

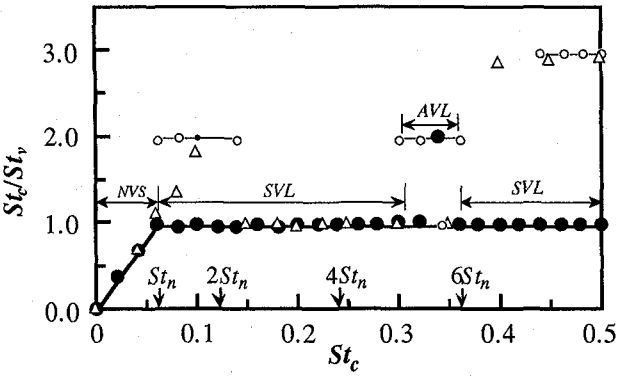

Fig.6. Variation of vortex shedding Strouhal number St_v along forced oscillatory Strouhal number St_c for B/H=2 cylinder under in-line oscillation at amplitude of a/H=14%; the symbols are used in the same way as in Fig.5

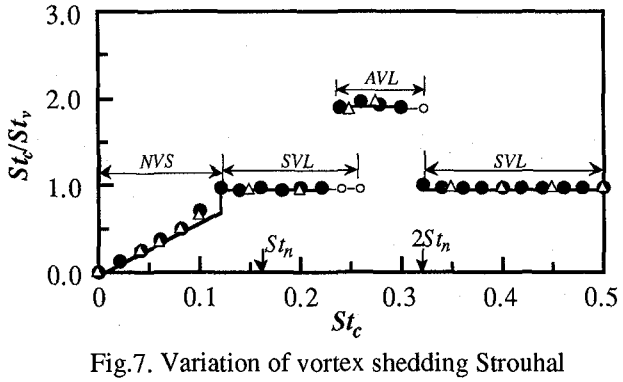

Fig.7. Variation of vortex shedding Strouhal number St_v along forced oscillatory Strouhal number St_c for B/H=3 cylinder under in-line oscillation at amplitude of a/H=14%; the symbols are used in the same way as in Fig.5

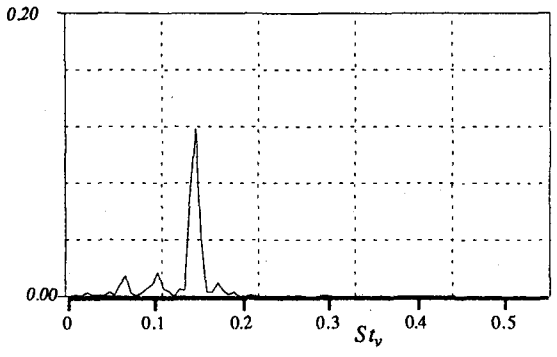

(a) St_c=0.08

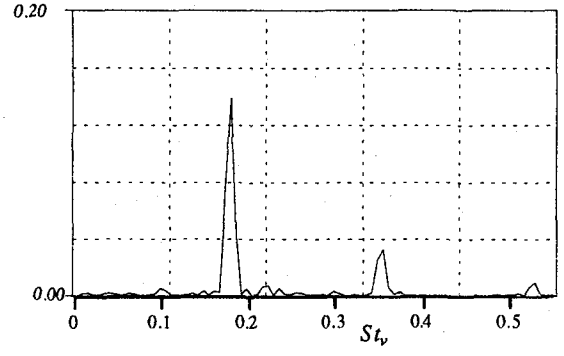

(b) St_c=0.34

Fig.8. Frequency spectra of lift signals from square cylinder oscillating at amplitude a/H=14% and at (a) St_c=0.08, (b) 0.34

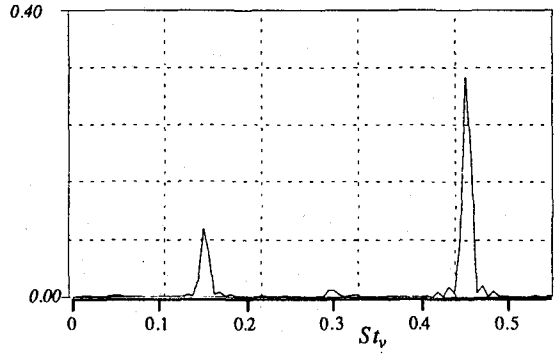

Fig.9. Frequency spectrum of lift signal from B/H=2 cylinder oscillating at amplitude a/H=14% and at St_c=0.44

Strouhal numbers St_v ($=f_vH/U$; f_v is vortex shedding frequency) along forced Strouhal numbers St_c for B/H=1, 2 and 3 cylinders under in-line oscillations of amplitude a/H=14%. The vortex-shedding frequencies f_v are obtained from the spectral frequency analyses of C_L signals. As C_L is dominantly determined by the shedding of vortices, the frequency of C_L is considered to stand for the frequency of vortex shedding in the wake. In the figures, the 1st peak, as well as the 2nd and 3rd peaks if apparent, in the frequency spectrum is shown. The simulated results are also given for comparison.

From Fig.5, it can be seen that the vortices mainly

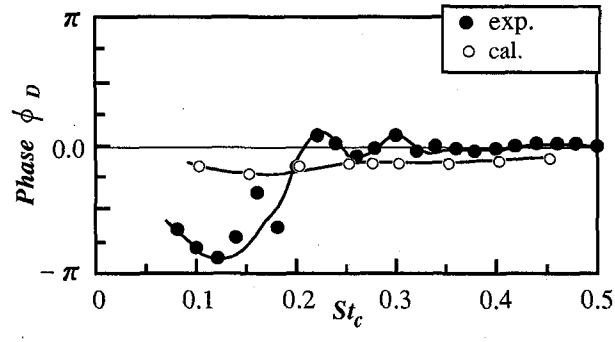

Fig.10. Phase angles of drag forces relative to cylinder displacements along forced oscillatory Strouhal number St_c for B/H=1 cylinder under in-line oscillation at amplitude of a/H=14%

shed in three different frequencies, based on which the wake flow features can be divided into three kinds as the forced Strouhal number St_c increases. One is the Natural Vortex Shedding (*NVS*) region, where dominant shedding frequency is the natural frequency (see Fig.8(a)). The other is the Symmetric Vortex shedding Lock-in (*SVL*) region, at about $0.1 \leqq St_c \leqq 0.14$ and $St_c \geqq 0.38$ as in Fig.5, in which the vortex shedding is synchronized with or locked into the forced oscillation in such a way that the vortices shed almost symmetrically in near-wake and thus in the same frequency with the forced one. The third is the Alternate Vortex shedding Lock-in (*AVL*) region, at about $0.2 \leqq St_c \leqq 0.36$ as in Fig.5, where the vortex shedding is locked into half of the forced frequency, i.e., each side of the cylinder sheds one vortex every two vibration cycles and forms alternate vortex street in the near-wake. The *AVL* region of square cylinder is centered at about double the natural Strouhal number St_n. It is well known that in the wake of a circular cylinder under in-line oscillation, the *AVL* region is also centered at double the natural Strouhal frequency.

From Figs. 6 and 7, it can be seen that there appear also *NVS*, *SVL* and *AVL* regions at different stages of forced oscillations. Of particular interests is that the *AVL* region is located at about St_c=0.33 for B/H=2 cylinder, although that of B/H=3 cylinder is still centered at about $2St_n$. From Otsuki et al.[11], it is known that the variation curve of natural Strouhal number St_n with the change of side ratio B/H has a jump at about B/H=2.8. Before the jump, the shear layers are fully separated from the afterbody and form alternate vortex street in the wake, while after the jump they reattach with the afterbody and then shed to the wake alternately. For cylinders with side ratios of from 2.0 to 2.8, however, the wake flow has another natural shedding tendency, which corresponds to reattaching flow patterns and is about St_n'=0.16 for B/H=2 cylinder. This second natural shedding frequency can be amplified under certain external excitations and results in reattached flow patterns. At *AVL* region in Fig. 6, the forced frequencies are about twice this second natural shedding frequency and thus trigger the reattached flow patterns.

If we compare Figs.5, 6 and 7 with Figs.2, 3 and 4, it

can be seen that the *AVL* region is dynamically characterized by the plateau values of C_D. For a circular cylinder under in-line oscillations, the lock-in range is not so wide, say, from f_c/f_n=1.55 to 2.5 at oscillatory amplitude of a/H=14%[2]. For a rectangular cylinder, however, the lock-in or synchronization range is much wider because its long afterbody, acting as a splitter plate, substantially weakens the interaction of upper and lower shear layers and makes difficult the formation of normal *Karman* vortices. Therefore the vortex shedding can be much more easily effected by the external disturbances. The lock-in or synchronization can be realized either in *SVL* mode or *AVL* mode.

It is very interesting that there is a phenomenon of frequency combination, as shown by the second or the third peaks at St_c/St_v=0.66 in the range of St_c between 0.2 and 0.34 in Fig.5. This range coincides well with the *AVL* region, where, as shown in Fig.8(b), in addition to the 1st peak (captured vortex shedding frequency, equal to half of the forced) and the 2nd peak (forced frequency), there is a 3rd peak which is a combination of the former two ($St_c/2+St_c$). As the forced frequencies roughly double the natural shedding frequencies in *AVL* region, i.e. $St_c/2=St_v$, it is actually the combination of two source frequencies, namely, the natural shedding frequency and the forced one. In a system composed of oscillating body and flow, there are mainly two source frequencies, namely natural vortex shedding frequency and the forced oscillatory frequency. When the forced frequency is near twice the natural one, there exists possibility for the combination of these two frequencies. This frequency combination phenomenon is also found by Minewitsch et al.[7] in their numerical simulations. For B/H=2 cylinder as shown in Fig.6, the second peaks at $St_c \geqq 0.44$ represent the one third component of forced frequency, of which a spectral distribution is shown in Fig.9 as an example.

One more thing that should be noted in Fig. 5 is that, at St_c=0.16 and 0.18, there occurs the so-called deviation phenomenon found by Barbi et al.[12]. In their experimental study of a circular cylinder in oscillatory flow, Barbi et al. found that, although it is universally accepted that bluff bodies shed vortices either at their natural frequency or at the frequency of the disturbance, or harmonic of it, the change from natural shedding to synchronized shedding is not in an abrupt way, but through a transient process in which the vortices are shed neither at natural frequency nor at harmonic of driving frequency but something between them. The present results confirm that this phenomenon also occurs for square cylinder although the separation points of flow is fixed.

The numerically simulated results (open triangle symbols) show a relatively good agreement with those of experiments, although for B/H=2 cylinder, the one third component seems to be dominant in high frequency range.

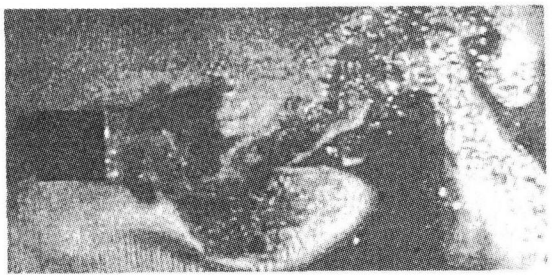

(a) St_c=0.15

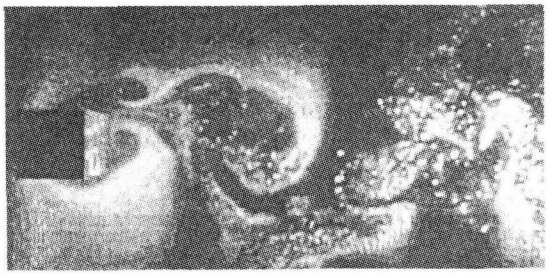

(b) St_c=0.2

(c) St_c=0.3

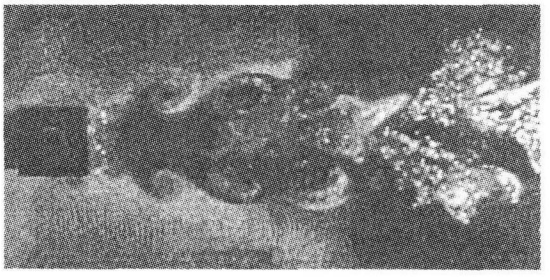

(d) St_c=0.45

Fig.11. Visualized flow patterns around a square cylinder oscillating longitudinally at (a) St_c=0.15, (b) 0.2, (c) 0.3 and (d) 0.45 and at amplitude a/H=14%; all photos are taken at the maximum upstream position during one cycle of oscillation

4.3. Aeroelastic features estimated from forced in-line oscillation test

Fig.10 shows the phase differences between the drag forces and body displacements for square cylinder under in-line oscillation of amplitude a/H=14%. Phase angle is defined as the angle by which the drag force leads the in-line displacement of the cylinder. As well known, a

(a) St_c=0.15

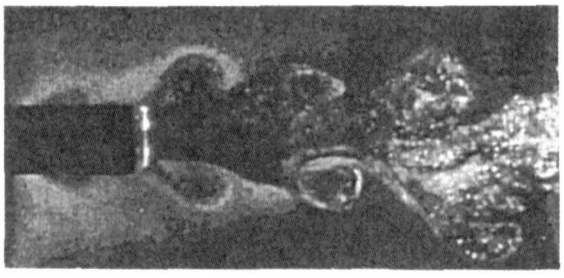

(b) St_c=0.2

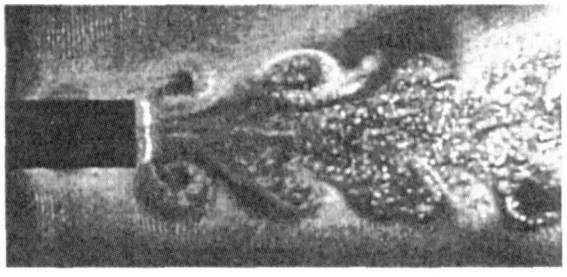

(c) St_c=0.3

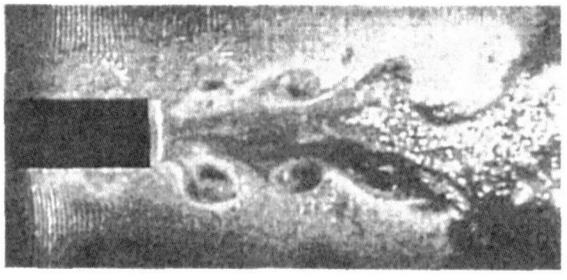

(d) St_c=0.45

Fig.12. Visualized flow patterns around a B/H=2 cylinder oscillating longitudinally at (a) St_c=0.15, (b) 0.2, (c) 0.3 and (d) 0.45 and at amplitude a/H=14%; all photos are taken at the maximum upstream position during one cycle of oscillation

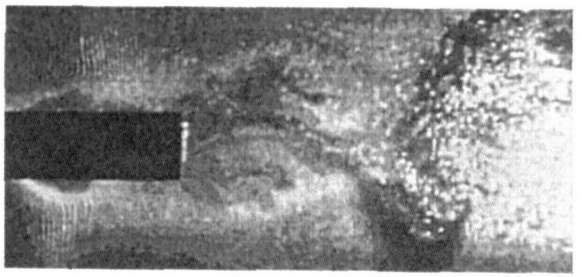

(a) St_c=0.15

(b) St_c=0.2

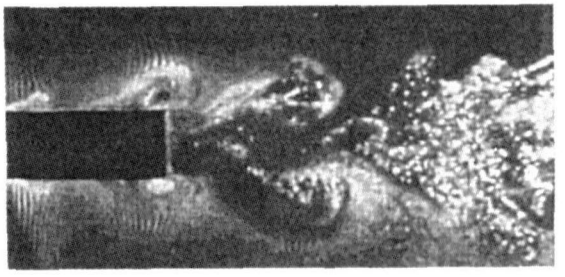

(c) St_c=0.3

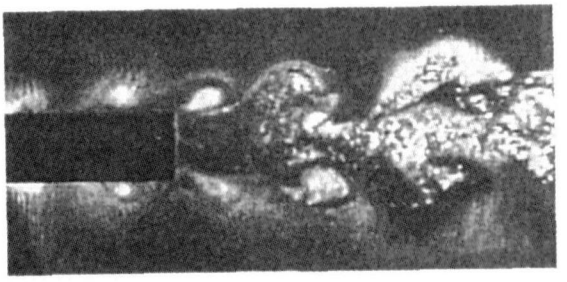

(d) St_c=0.45

Fig.13. Visualized flow patterns around a B/H=3 cylinder oscillating longitudinally at (a) St_c=0.15, (b) 0.2, (c) 0.3 and (d) 0.45 and at amplitude a/H=14%; all photos are taken at the maximum upstream position during one cycle of oscillation

positive phase angle means the intensifying of oscillation and thus indicates unstable feature, and a negative phase means stable feature. The experimental results show that at about $St_c \leqq 0.22$, the flow shows stable features; namely, the cylinder would not experience sustained in-line oscillation if permitted for free oscillation. In the region about $0.23 \leqq St_c \leqq 0.34$, however, there exist two small ranges where phase angles are in positive values; namely

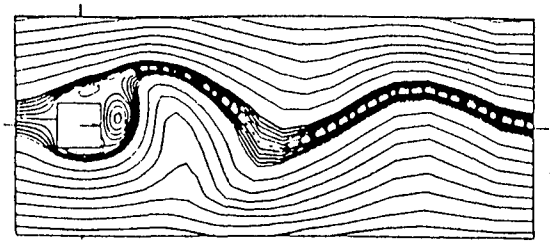

(a) St_c=0.15

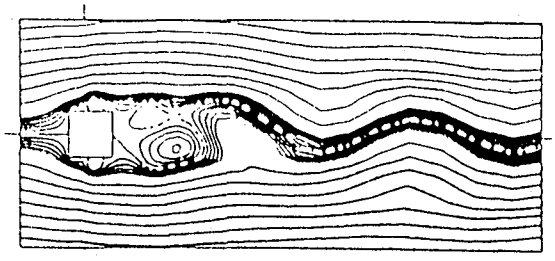

(b) St_c=0.45

Fig.14. Simulated streamlines around B/H=1 cylinder under in-line oscillations at amplitude of a/H=14%; the streamlines are taken at the maximum upstream position during one cycle of oscillation

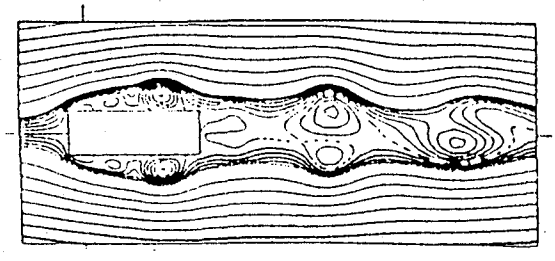

(a) St_c=0.15

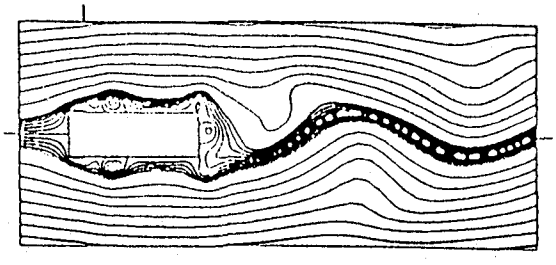

(b) St_c=0.3

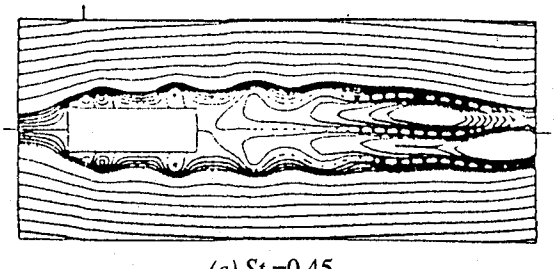

(c) St_c=0.45

Fig.15. Simulated streamlines around B/H=3 cylinder under in-line oscillations at amplitude of a/H=14%; the streamlines are taken at the maximum upstream position during one cycle of oscillation

there are possibilities for the cylinder to develop sustained free oscillation there. Naudascher[4] did report, in his review on free in-line oscillation tests of rectangular cylinders, that there appear two regions from St_c=0.2 to 0.33 for the square cylinder, where the cylinder may oscillate freely at very small amplitude of a/H=4.5%, a much smaller value than the present forced amplitude. It should be noted that the numerical simulations, also of at forced amplitude of a/H=14%, predict a more stable features than experiments. To evaluate the effects of oscillatory amplitude on the aerodynamic characteristics, further simulations on much lower amplitudes are needed in the future.

5. Visualized flow patterns

The three cylinders are made to oscillate in-line with an incident flow at forced Strouhal numbers St_c=0.15, 0.2, 0.3, and 0.45 respectively and at an amplitude of a/H=14% in visualization. Figs.11, 12, and 13 show the visualized flow patterns for B/H=1, 2 and 3 cylinders respectively, with all photos taken at the maximum upstream position during one cycle of cylinder motion. Parts of the visualized results were reported in Okajima et al.[13].

We examine the photos of square cylinder at first. From Fig. 11, it can be seen that, at St_c=0.15, although a pair of small symmetric vortices is formed right after leading edges, it immediately switches to asymmetric vortices as soon as it sheds from the trailing edges. The shear layers forming the vortices are mainly from the front separation points. The "wake swing" is evident, and the width of wake is about four times of the height (H). From Figs.11(b), (c) and (d), it can be seen that, for all the cases, a pair of symmetrical vortex forms along the side surfaces and rolls up to shed downstream symmetrically; the symmetric wake finally develops into antisymmetric vortex street; but with the increase of forced Strouhal number, the symmetric part of wake keeps longer. Furthermore, the width of wake becomes apparently narrow as the St_c of oscillation increases.

As well known, the flow passing a stationary cylinder, either circular or rectangular cylinder, has an inherent or natural tendency to form an asymmetric mode of vortex shedding. On the other hand, when a cylinder is forced to oscillate in-line with the incident flow, the in-line motion imposes a symmetric perturbation to the flow. The interaction of these two effects is responsible for the dynamic characteristics and flow structures. Whether or not the symmetric modes of vortex shedding will prevail in the wake depends on whether or not the effect of forced perturbation on flow can overwhelm the inherent tendency of flow. Therefore, at high ratios of St_c/St_n (or f_c/f_n), the wake tends to become more symmetric and more narrow.

For B/H=2 rectangular cylinder, Fig.12 shows the visualized flow patterns at (a) St_c=0.15, (b) 0.2, (c) 0.3, and (d) 0.45. It is worthy noting that, as St_c/St_n of B/H=2 cylinder is much higher than that of square cylinder at the same St_c, the wake from the former is much more

symmetric than that of the latter at the same St_c. This confirms the above discuss that at high ratios of St_c/St_n (or f_c/f_n), the wake tends to become more symmetric and more narrow. Furthermore, Fig.13 shows the visualized flow patterns from the B/H=3 rectangular cylinder vibrating longitudinally at (a) St_c=0.15, (b) 0.2, (c) 0.3, and (d) 0.45. The same trend that the symmetry of vortex shedding increases and the width of wake decreases with the increase of St_c is found here again.

It should be emphasized here that, although the two distinct vortex shedding modes, i.e. antisymmetric and symmetric shedding, appear only singly in two distinct regions of excitation in the free-oscillation tests of circular cylinder[9], the performances of these two modes in forced in-line oscillations of a rectangular cylinder are quite different. In the present visualization, we found that, as St_c/St_n increases, the change of flow structures from antisymmetric to symmetric is in such a way that the symmetric part of the wake increases gradually although the far wake is still antisymmetric. More important is that the wake flow is very unsteady, with the two vortex shedding models always appearing intermittently. Even at high forced frequencies, although the vortex shedding keeps symmetric in the near wake, the intermittent appearance of symmetric and antisymmetric vortex street is observed in the middle or far wake.

6. Some remarks on the comparison of simulations and experiments

As mentioned early, there do exist some discrepancies between the experimental and simulated results as shown in Figs. 2-7 and Fig.10, especially for lift forces. The main reasons responsible for this discrepancies are supposed to be the existence of intermittent appearance of symmetric and antisymmetric vortex shedding and the existence of three dimensionality in the experiments. From Fig.2, it can be seen that the simulated C_L values are much larger than those of experiments in the range of about $St_c \leqq 0.25$, just where the vortices always shed alternately either in natural shedding frequency (in *NVS* region) or in half of the forced frequency (in *AVL* region) as shown in Fig. 5. On the other hand, at range of $St_c \geqq 0.25$ where the vortices gradually shift to shed symmetrically (in *SVL* region), the simulated C_L values are much smaller than the experimental values. Checking Figs. 3 and 4 together with Figs. 6 and 7, we can also observe this correspondences between the lift forces and vortex shedding modes (Note the *AVL* region of B/H=2 cylinder doesn't appear at simulations). That is, within a range where the vortices are supposed to shed in alternate or symmetric shedding mode, the simulated lift forces tend to be larger or smaller than the experimental values.

It was reported that the three dimensionality and the turbulences begin to appear in the wake flow of a bluff body at Reynolds numbers as low as Re=200. At $Re=4\times10^3$ as in this experiments, the wake flow from an oscillating rectangular cylinder is sure to be both three dimensional and turbulent. On the other hand, in the present numerical simulations, the flow at $Re=1\times10^3$ is supposed to be two-dimensional and laminar. Under certain forced frequencies, strictly symmetric flow patterns appear in simulations, resulting in the almost zero values of lift forces as shown in Figs.3, 4 and 5. Under other conditions, the simulations predict singly and uniformly alternate vortex shedding, resulting in a larger values in lift forces. As an example, Fig.14 gives two kinds of simulated flow patterns for square cylinder. Furthermore, Fig.15 shows the simulated flow patterns of B/H=3 cylinder, which are symmetric at (a)St_c=0.15, (c)0.45 corresponding to the two bottom values of C_L curve, and antisymmetric at (b)0.3 corresponding to the peak values. It is worthy noting that in the far wake of Fig.15(a) and (c), the vortex shedding switches from symmetric to antisymmetric.

In experiments, however, the vortex shedding behaves much less extremely; it seldom sheds the strictly symmetric flow patterns or singly and uniformly alternate vortex street all the time. Instead, the visualization shows that the two vortex shedding modes, the symmetric and antisymmetric, tend to appear and replace each other intermittently in the wake, although the dominant mode agrees well with simulations as in Figs. 5, 6 and 7. In Figs.11, 12 and 13, we only show the dominant shedding modes. Even at high forced frequencies, such intermittent appearance and replacement of the two modes occur in the middle or far wake. Therefore, the average values of measured lift forces seldom change greatly and only increase a little at very high forced frequencies.

For the flow around a rectangular cylinder under transverse oscillation, it is confirmed that the three dimensional simulations obtained much closer results to experiments than the two dimensional simulations[14]. Now the same job is on the way for rectangular cylinder under in-line oscillations. It is expected that three dimensional simulations will have a much better accuracy in approaching to experiments than the two dimensional simulations.

7. Conclusions

Experimental measurements on the mean drags C_D and the *rms* lifts C_L acting on a rectangular cylinder under in-line oscillations, and the associated vortex shedding frequencies St_v and phase angles of drags to cylinder displacements ϕ_D are reported in this paper. Also shown are the visualized flow patterns of the wake flows. It is shown that both C_L and C_D don't have sharp changes which are experienced by a circular cylinder under in-line oscillation. Instead, the C_D values only show some small increases corresponding to the *AVL* region, and C_L values increase a little at very high forced frequencies.

By spectrally analyzing the experimental lift signals, the vortex shedding frequencies are obtained. It is found that, as St_c increases, the wake flow can be divided into *NVS* region, *AVL* region and *SVL* region. The vortices can shed in different combinations of natural shedding frequency f_n and forced oscillatory frequency f_c, and can

easily locked into *AVL* and *SVL* regions. The synchronization range includes both *AVL* and *SVL* and is much wider than that of a circular cylinder.

The effects of in-line oscillations on the vortex shedding can be expressed by St_c/St_n. The higher the value of St_c/St_n is, the more predominant the symmetric mode will be in the vortex shedding. However, as shown in visualization, the wake flow of a rectangular cylinder under in-line oscillations is characterized by the intermittent appearance of the symmetric and antisymmetric vortex shedding. Such characteristics, together with three dimensionality, are supposed to be responsible for the discrepancies between the experimental and simulated lift forces. In two-dimensional simulations, either strictly symmetric flow pattern or alternate vortex shedding is predicted. Therefore, within a range where the simulated vortices shed in alternate/ symmetric shedding mode, the simulated lift forces tend to be larger/smaller than the experimental values.

References

(1) Tanida, Y , Okajima, A. and Watanabe, Y., Stability of a circular cylinder oscillating in uniform flow or in a wake, *Journal of Fluid Mechanics*, Vol.61, part 4, pp.769-784, 1973.

(2) Grifffin, O. W. and Ramberg, S. E., Vortex shedding from a cylinder vibrating in line with an incident uniform flow, *Journal of Fluid Mechanics*, Vol.75, part 2, pp. 257-271, 1976.

(3) Knisely, C., Matsumoto, M. and Menacher, F., Rectangular cylinders in flows with harmonic perturbations, *Journal of Hydraulic Engineering, ASCE*, Vol.112, No.8, August, 1986.

(4) Naudascher, E., Flow-induced streamwise vibrations of structures, *Journal of Fluids and Structures*, Vol.1, pp.265-298, 1987.

(5) Ongoren, A. and Rockwell, D., Flow structure from an oscillating cylinder, Part II. Mode competition in the near wake, *Journal of Fluid Mechanics*, Vol.191, pp.225-245, 1988.

(6) Okajima, A. and Kitajima, K., Numerical study on aeroelastic instability of cylinders with circular and rectangular cross-sections, *Journal of Wind Eng. & Indust. Aerodyn.*, Vol.46&47, pp.541-550, 1993.

(7) Minewitsch, S., Franke, R. and Rodi, W., Numerical investigation of laminar vortex-shedding flow past a square cylinder oscillating in line with the mean flow, *Journal of Fluids and Structures*, Vol.8, pp.787-802, 1994.

(8) King, R., Prosser, M. J. and Johns, D. J., On vortex excitation of model piles in water, *Journal of Sound and Vibration*, Vol.29, pp.169-188, 1973.

(9) King, R., Hydroelastic model tests of marine piles, *British Hydromechanics Research Association Report*, RR 1254, 1974.

(10) Okajima, A., Yi, D., Kobe, M. and Ueno, H., Numerical and experimental studies on fluid dynamic forces of an oscillating rectangular prism, *Proceedings of the 1994 joint ASME/JSME pressure vessels and piping conference*, Minneapolis, Minnesota, USA, PVP-Vol.273, pp.257-264, 1994.

(11) Otsuki, Y., Washizu, K., Tomizawa, H. and Ohya, A., A note on the aeroelastic instability of a prismatic bar with square section, *Journal of Sound and Vibration*, Vol.34(2), pp.233-248, 1974.

(12) Barbi, C., Favier, D.P., Maresca, C.A., and Telionis, D.P., Vortex shedding and lock-on of a circular cylinder in oscillatory flow, *Journal of Fluid Mechanics*, Vol.170, pp.527-544, 1986.

(13) Okajima, A., Yi, D., Kobe, M. and Ueno, H., Observations of flows about a longitudinally oscillating cylinder with rectangular cross-section, *Proceedings of the Third Asian Symposium on Visualization* (eds. Nakayama, Y. and Tanahashi, T.), pp.63-68, Chiba, Japan, 1994.

(14) Okajima, A. and Yi, D., Three dimensional numerical computations of flows around stationary and oscillating cylinders, *Proceedings of the 1995 joint ASME/ JSME pressure vessels and piping conference*, Honolulu, Hawaii, USA, PVP-Vol.311, pp.73-80, 1995.

(Received September 18, 1995)